Controlling Hydrogenation of Graphene on Transition Metals

**M. L. Ng,[†,‡] R. Balog,[§] L. Hornekær,[§] A. B. Preobrajenski,*[,‡] N. A. Vinogradov,[†,‡]
N. Mårtensson,[†,‡] and K. Schulte*[,‡]**

*Department of Physics, Uppsala University, Box 530, 75121 Uppsala, Sweden; MAX-lab, Lund University,
Box 118, 22100 Lund, Sweden; and Department of Physics and Astronomy and Interdisciplinary Nanoscience
Center (iNano), Aarhus University, 8000 Aarhus C, Denmark*

A monatomic layer of graphite (MG or graphene) adsorbed on the (111) faces of transition metals Pt, Ir, and
Ni, has been employed for controlling the atomic hydrogen adsorption site selectivity and the amount of
hydrogen adsorbed upon saturation. The variations in the graphene-metal chemical bonding caused by
hydrogenation and the values of saturated hydrogen coverage have been studied by X-ray photoemission and
X-ray absorption spectroscopy. The hydrogenation of the graphene/metal systems has also been compared to
the hydrogen adsorption on highly oriented pyrolytic graphite under the same experimental conditions. It has
been found that graphene adsorption on the transition metal substrates can drastically enhance the hydrogen
uptake values. The highest values have been observed for MG/Ir(111), less for MG/Pt(111), even less for
MG/Ni and the least for the adsorption on bulk graphite. The high level of H coverage on MG/Ir and MG/Pt
has been assigned to the preferential H adsorption on the more bonding patches (pores) of the MG/metal
coincidence lattice. This adsorption creates unpaired electrons which contribute to a strengthening of the
graphene-metal bonds. In this way, the densest possible graphane-like patches can be formed on MG/Pt and
MG/Ir. On the MG/Ni interface the formation of graphane is obstructed by the strong interfacial bonding.

Introduction

Graphene or monolayer graphite (MG) offers tantalizing
opportunities in the relentless race toward smaller and faster
electronics due to its two-dimensional structure and excellent
electron mobility.[1,2] A controllable band gap opening, however,
is a precondition, which needs to be achieved before graphene
can be utilized in e.g. carbon-based electronics. In addition,
graphene is a suitable material for chemical vapor sensing, since
its electrical properties are very sensitive to adsorption of various
molecules.[3] It has been shown that electronic changes in
graphene can be realized by means of controllable chemical
functionalization.[4] In particular, hydrogenation of graphene
offers an elegant route toward tailoring electronic (metal-
semiconductor transition) and magnetic (nonmagnetic-ferro-
magnetic) properties of graphene,[5–10] as well as providing the
opportunity for hydrogen storage.[11,12]

Experimental investigations of hydrogenation of graphene
have revealed very different structural behavior on supported
and free-standing graphene. On SiC supported graphene, the
adsorption of individual H atoms results in the formation of
coadsorbed pairs of H atoms on either neighboring C atoms
(1,2-dihydrogenated ring, ortho-dimer) or opposite C atoms (1,4-
dihydrogenated ring, para-dimer) in the graphene ring.[13] Al-
though at very low coverage dimers preferentially form on the
protruding areas of a graphene sheet modulated by the underly-
ing 6 × 6 reconstruction, with increasing coverage, of hy-
drogen atoms tend to cluster in a rather disordered manner.[13]
Therefore, the hydrogen structures formed on the SiC supported
graphene very much resemble those known on the graphite

surface.[14] However, results from experiments with hydrogen
treated free-standing graphene indicate the formation of a
graphane structure.[8] Here, a dense packing of one hydrogen per
carbon placed on alternating sides of the sheet for adjacent
carbon atoms forms a highly stable regular arrangement through
sp^3 hybridization.[11] Recently, similar sp^3 configuration has been
observed on Ir(111) supported graphene, where a C−H bond
at the MG−Ir interface is substituted by the formation of a
strong C−Ir bond.[10] Moreover, the hydrogenation of graphene
on Ir(111) generates a highly regular hydrogen pattern, giving
rise to a large gap opening at the Fermi level. From these
experimental findings, it is clear that the interaction of hydrogen
with graphene strongly depends on the underlying substrate and
on whether only one or both sides of the graphene sheet are
chemically active. An important question is then, how the
strength of the chemical interaction between MG and the
underlying substrate modifies the hydrogen reactivity. This issue
can be addressed by studying hydrogenation of graphene on
several different transition metal (TM) substrates with varying
strength of the interfacial interaction. In addition, graphene layers
formed on transition metals are often naturally and periodically
nanostructured due to a combination of the MG/TM lattice
mismatch and a certain strength of chemical bonding[15,16] thus,
offering nanoscale regions with different hydrogen reactivity
in the same MG/TM system.

In the present work, we compare the hydrogenation processes
for graphene grown on Pt(111), Ir(111), and Ni(111). The
strength of interaction between graphene and the substrates is
increasing in the series Pt−Ir−Ni[15] providing a possibility to
correlate it with the hydrogen uptake. For comparison, we
present the case of highly oriented pyrolytic graphite (HOPG)
hydrogenated under the same conditions as the MG/TM
interfaces. Since there is no significant chemical interaction
between the atomic layers in HOPG, this reference experiment

* To whom correspondence should be addressed: E-mail: alexeip@
maxlab.lu.se; karina.schulte@maxlab.lu.se.
† Department of Physics, Uppsala University.
‡ MAX-lab, Lund University.
§ Department of Physics and Astronomy, Aarhus University.

allows us to demonstrate the general impact of the metal substrates on the hydrogenation process. The characterization of the samples is performed by a combination of core-level photoelectron spectroscopy (PES), near-edge X-ray absorption fine structure (NEXAFS) spectroscopy and low energy electron diffraction (LEED). With these techniques we reveal the influence of the MG/TM interface reactivity on the total hydrogen uptake and study site selectivity of the hydrogen adsorption.

Experimental Section

All samples were prepared in situ at beamline D1011, MAX-lab, Lund University. The single crystal substrates Pt(111), Ir(111), and Ni(111) were cleaned with several cycles of Ar^+ sputtering, annealing and oxygen treatment (whenever necessary). A single monolayer of graphene was prepared by thermal cracking of propylene molecules on the hot crystal surface, i.e., 650 °C on Pt, 780 °C on Ir, and 670 °C on Ni for 30 min in the propylene partial pressure of $3-5 \times 10^{-8}$ mbar. The presence of MG was checked by the core level intensity ratios in PES and confirmed by LEED patterns characteristic for just one atomic layer of graphene. The HOPG sample was cleaved in situ and annealed to 600 °C. The samples were hydrogenated at room temperature (RT) by atomic hydrogen from an Omicron EFM H source oriented normal to the substrate surface. To reach hydrogen saturation, we operated the source at $T = 2200$ K (30 mA at 1 kV) in a hydrogen gas partial pressure of 1.0×10^{-7} mbar for 15 min. The saturation level was confirmed by PES, i.e., no further changes occurred to the spectra with increasing H exposure at this source temperature. Furthermore, the saturation level for MG on Pt, Ir, and HOPG was also checked at higher source temperature, i.e., 2600 K, but no perceptible changes could be observed. Only the samples fully hydrogenated to saturated coverage are discussed throughout this work. All samples were characterized by core level PES, NEXAFS, and LEED. The LEED results are not discussed in the following because no ordered surface symmetry was detected, implying that H adsorption occurred randomly. The C 1s NEXAFS spectra were measured in partial electron yield (PEY) mode ($U = -100V$) for higher surface sensitivity. The photon energy resolution for NEXAFS at the C K-edge was set to 75 meV. The PE spectra were accumulated in normal emission at a resolution of 125 meV. All NEXAFS spectra were normalized to spectra from the clean metal surfaces. The core level PE spectra were measured relative to the Fermi level and deconvoluted using the FitXPS software.[17]

Results and Discussion

Figure 1 depicts the C1s NEXAFS of pristine (black curves) versus H-saturated (red curves) HOPG and MG on Pt, Ir, and Ni. Prior to hydrogen treatment, we observe a common trend of increasingly perturbed electronic structure at the C K-edge in the sequence of HOPG−MG/Pt−MG/Ir−MG/Ni.[15] The original features A, B, and C, which are signatures of the π^*, σ_1^*, and σ_2^* states respectively, are most distinctive in the spectrum of clean HOPG (Figure 1a). For graphene on the 5d metals, peak A has gained an additional shoulder A_1 while peaks B and C have become broader, although the overall spectral shape is preserved (Figure 1b,c). For the MG/Ni case (Figure 1d), another peak A_2 has appeared, whereas peaks B and C are completely smeared out. This signifies that the MG−Ni interaction is of a strong chemical nature. Therefore, the interaction between the top layer graphene and the substrate is growing from physisorption (HOPG) to weak chemisorption (MG/Pt and
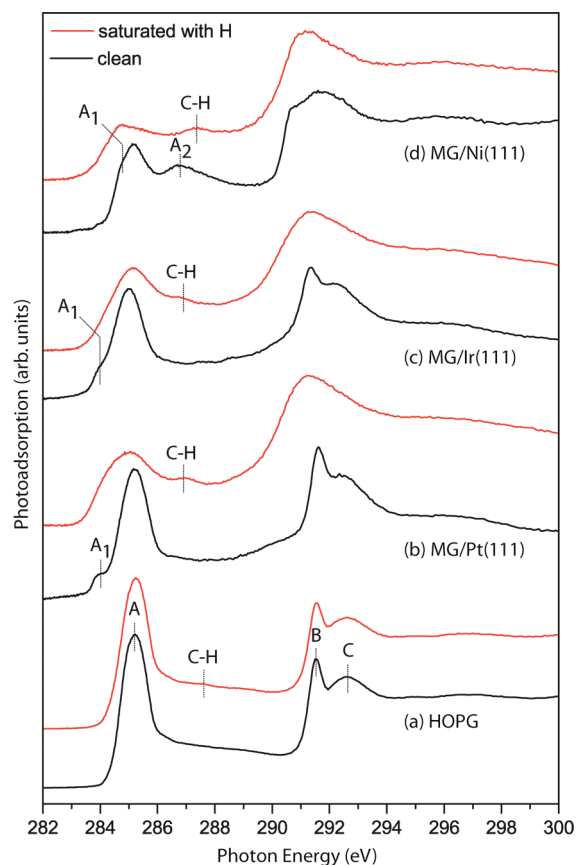

Figure 1. The C 1s NEXAFS spectra from the pristine (black curves) and the hydrogen saturated (red curves) samples. The angle of incidence is 50 °C in all cases. (a) HOPG, (b) MG on Pt(111), (c) MG on Ir(111), and (d) MG on Ni(111).

MG/Ir) and finally to strong chemisorption (MG/Ni). For the lattice-mismatched systems (MG/Pt and MG/Ir), the periodic alternation of favorable and unfavorable adsorption sites results in a weak periodic corrugation of graphene with a period of several nanometers. In this work, we will refer to the low lying (more bonding) parts as "pores" and to the elevated (less bonding) parts as "wires". Since the MG−Ir bond is stronger than that of MG−Pt, the corrugation of graphene is somewhat more pronounced on Ir(111) than on Pt(111).[15]

Upon hydrogenation, the spectrum of HOPG (Figure 1a) is virtually unchanged, except for the appearance of a minor peak at 287.5 eV commonly associated with the C−H bonds in the C 1s NEXAFS of hydrocarbons.[18] The robustness of the C 1s NEXAFS shape of HOPG upon hydrogenation is due to the fact that atomic hydrogen does not intercalate into graphite, but chemisorbs on the topmost layer only.[14,19] Since several graphitic layers contribute to the signal, it is hard to determine how much the electronic structure of the topmost layer is affected by hydrogenation. In contrast, adsorption of hydrogen on the MG/TM systems results in an obvious change of the spectral shape (Figure 1b,c) indicating a significant modification of the graphene electronic structure. All features are broadened, the π^* state intensity is lowered, the C−H peak is more pronounced, and the energy separation between the π^* and σ^* manifolds is reduced for the case of Pt and Ir. All of these changes indicate that the carbon atoms form chemical bonds with hydrogen. The reduced $\pi^*−\sigma^*$ separation for the H/MG/Pt and H/MG/Ir interfaces as compared to their non-hydrogenated counterparts implies weakening of the in-plane C−C bonds upon hydrogenation. This is understandable because hydrogen reacts with the
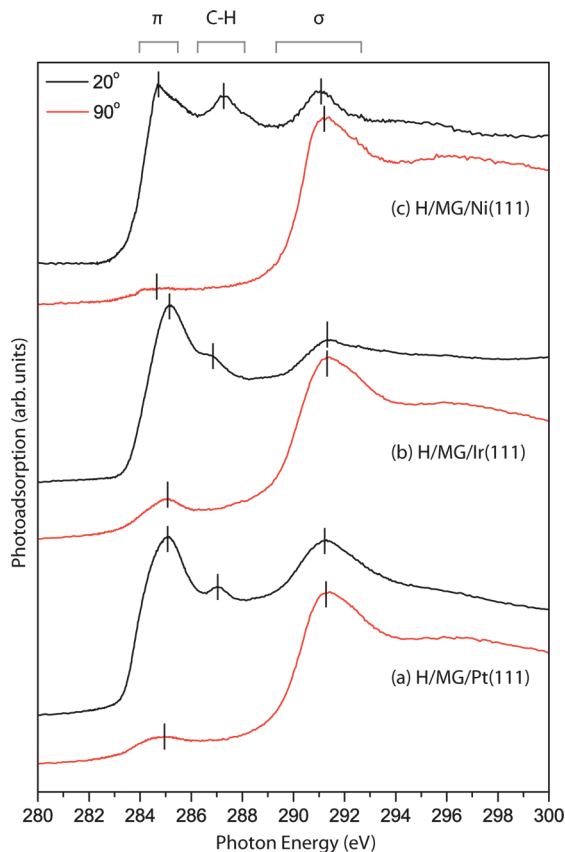
Hydrogenation of Graphene on Transition Metals

J. Phys. Chem. C, Vol. 114, No. 43, 2010 **18561**

Figure 2. Angle-resolved C 1s NEXAFS spectra of hydrogenated graphene on (a) Pt(111), (b) Ir(111), and (c) Ni(111).

basal plane which results in double bond breakage. For MG/Ni, the in-plane C−C bonds are already weakened in the pristine layer due to the strong chemisorption. In none of the MG layers does the π^* state intensity vanish entirely, signifying the presence of a certain amount of unhydrogenated graphene patches in all cases.

The orientation of the C−H bonds relative to the surface can be estimated by recording the NEXAFS spectra at different angles. In Figure 2, we show angle dependent C 1s NEXAFS spectra from different H/MG/TM interfaces measured with θ at 20 °C (grazing incidence) and 90° (normal incidence), where θ is the angle between the polarization vector of the light and the surface normal. From these spectra, it is apparent that the C−H bonds are oriented perpendicular to the graphene plane for all three interfaces, as no signature of these bonds is detected at normal incidence. A small tilt of the C−H σ^* bonds accompanying the formation of H−H dimers cannot be entirely excluded, but it is below the detection limit in our measurements. It should be noted, however, that if the graphene flakes would have been too small (or their defect density too large), the contribution from flat lying C−H bonds at the flake boundaries would become important and would also result in C−H related intensity at normal incidence.

Information about the exact hydrogen uptake values and the H adsorption positions can be obtained by analyzing high-resolution core level PES data. Figure 3 shows the carbon core level photoemission of the HOPG and MG layers on Ir and Pt before and after hydrogenation to saturated coverage. In the schematic drawings, the large gray circles represent metal atoms while the medium (colored) circles represent carbon atoms with various chemical environments in the graphene layer. Each color symbolizes a specific chemical state related to the components in the PE spectra. The small black circles are hydrogen atoms.
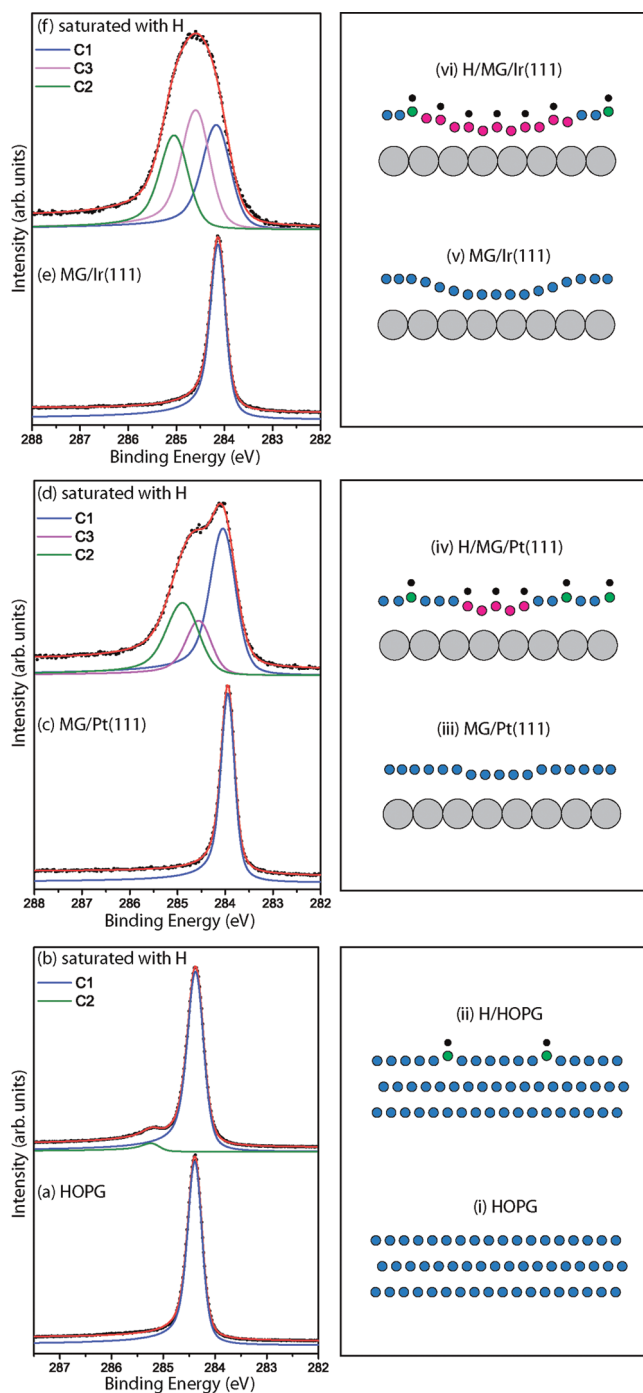

Figure 3. C 1s PES taken with $h\nu = 400$ eV (left) and the respective schematic drawings (right) of pristine and hydrogen saturated HOPG and MG on Pt(111) and Ir(111) [from bottom to top].

For clean HOPG (Figure 3a), the core level spectrum consists of a single component at 284.4 eV, accounting for the carbon species with the sp^2 bonds. Similarly, the spectra for the weakly hybridized graphene on Pt and Ir (Figure 3c,e) have only one component each despite the weak corrugation caused by the lattice mismatch.[15] The degree of graphene corrugation on Pt is slightly lower than on Ir,[15] as shown schematically in Figure 3(iii,v). On Ni, MG is strongly adsorbed and lattice matched, implying no nanoscale corrugation. Instead, the C atoms are located in an alternating manner on top of the Ni atoms and in fcc hollow sites, thus giving rise to an atomic scale rippling[20,21] (see Figure 5, i).

In general, the hydrogenation process can be categorized according to the sample reactivity, namely nonactivated graphene

TABLE 1: A Summary of Binding Energies for All Components in the C 1s PE Spectra

surface	component	BE (eV)
H/MG/Ni	dissolved C	283.2
	c3	284.2
	c1	284.7
	c2	285.3
MG/Ni	dissolved C	283.2
	c1	284.8
H/MG/Ir	C1	284.1
	C3	284.6
	C2	285.0
MG/Ir	C1	284.1
H/MG/Pt	C1	284.0
	C3	284.5
	C2	284.9
MG/Pt	C1	283.9
H/HOPG	C1	284.4
	C2	285.2
HOPG	C1	284.4

(HOPG), activated and weakly corrugated graphene (on Pt and Ir) and strongly activated and lattice matched graphene (on Ni). For the HOPG sample, the contribution of the topmost layer to the total C 1s signal is determined as $1 - \exp(-d/\lambda)$, where $d = 3.2$ Å is the interlayer distance and $\lambda = 4.5$ Å is the inelastic mean free path of the electrons,[22] giving approximately 50%. The peak at $E_B = 285.2$ eV (Figure 3(b)[green]) is interpreted as the C−H bond, in agreement with ref 19. By comparing the area under the C−H and the C=C components, we obtain a rather low saturated hydrogen uptake value of only 12% for HOPG, which is much lower than the value reported previously in ref 19 (37%). Further increase in the source temperature did not result in the increased H coverage in our experiments. In part, this discrepancy can be due to a different defect density for different HOPG samples or due to differences in sample preparation.

For the weakly bound MG/Ir and MG/Pt interfaces, the hydrogenation results in a redistribution of the spectral intensity in favor of the new components at higher BE (Figure 3d,f). The spectral shape can be reliably fitted for both cases by a minimum of three peaks, though more components cannot be excluded. All BEs are summarized in Table 1. The components at higher binding energies are assigned to sp^3 hybridized C atoms. On the basis of the relative peak areas, the total ratio of sp^3 to sp^2 C atoms is estimated to be as high as 50% for H/MG/Pt and 67% for H/MG/Ir and is thus much larger than the amount of hydrogenated carbon atoms on our reference graphite surface. Since all investigated substrates are treated with atomic hydrogen under identical conditions, the obtained values indicate that the hydrogenation process is considerably altered by the presence of the underlying TM substrate. In order to get insight into the nature of this effect, we consider in the following how graphene hydrogenation is reflected in the spectra of metal substrates.

Figure 4 shows the Pt and Ir 4f core level spectra for MG/Pt and MG/Ir before and after hydrogenation. Before the H treatment, both Pt and Ir 4f spectra consist of the bulk component at higher BEs and the interface component at lower BEs. Their shapes are nearly identical to that from the pristine Pt(111) and Ir(111) surfaces (not shown), confirming a weak interaction between MG and these two metal surfaces. Upon hydrogenation, the spectral shape is drastically changed. In the Pt 4f spectrum, the interface component (originally at 70.55 eV) is greatly reduced, while a new peak at 71.4 eV appears. Thus, the adsorption-induced shift to higher energies is as large
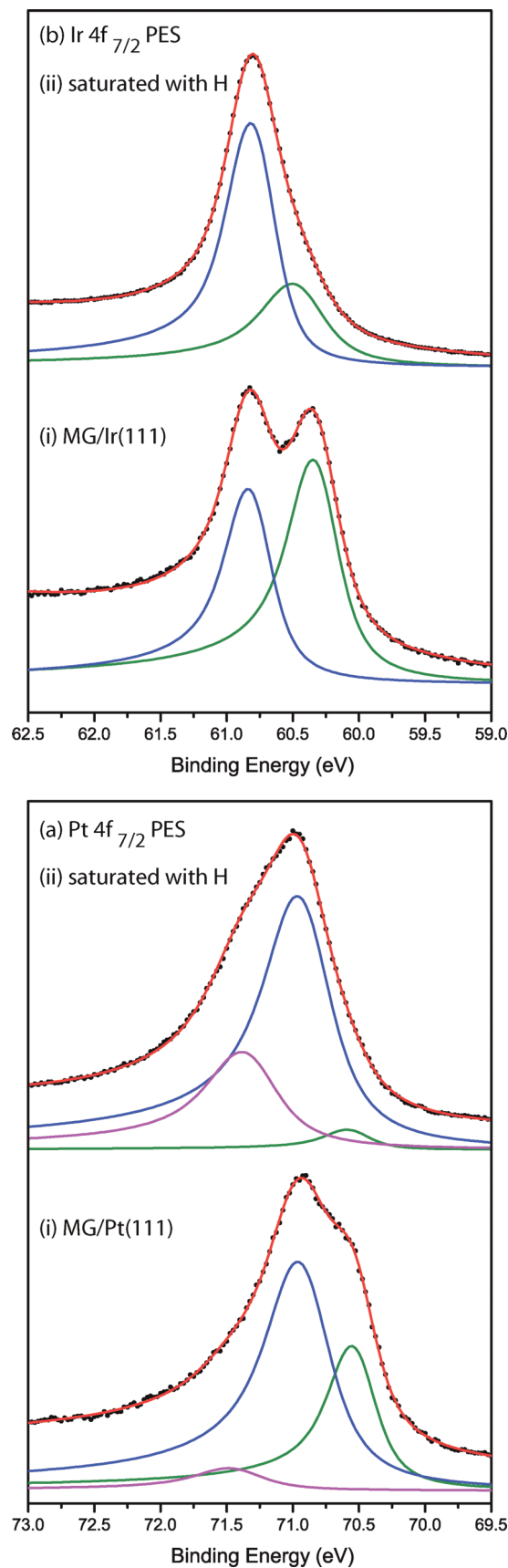
Figure 4. Pt 4f$_{7/2}$ PES ($h\nu = 150$ eV) and Ir 4f$_{7/2}$ PES ($h\nu = 120$ eV) of MG/Pt(111) and MG/Ir(111) before and after saturated H adsorption.

as 0.85 eV. This implies that the 5d dangling bonds of the topmost Pt layer are now interacting strongly with the graphene

Hydrogenation of Graphene on Transition Metals

J. Phys. Chem. C, Vol. 114, No. 43, 2010 **18563**

layer and the corresponding 5d electrons are transferred to the newly formed states resulting in the higher BEs. We have verified that the new component at 71.4 eV is not due to the formation of direct Pt−H bonds through hydrogenation of the pristine Pt(111) surface. However, it should be noted that a weak peak at 71.5 eV in the Pt 4f spectrum is visible even before hydrogenation (Figure 4a), probably as a consequence of the C−Pt bonding on grain boundaries and other sites with reduced carbon coordination. On Ir, the situation upon hydrogenation is similar (Figure 4b) albeit that the shift of the interface component is smaller than on Pt. Although the spectrum is fitted with only two components, the real situation is probably more complex due to the fact that different C atoms across the pore form bonds of different strength with the surface Ir atoms. The resulting Ir 4f spectrum contains a superposition of interface components with BEs that can range from 60.5 eV (low-energy component in our fit) to 60.8 eV (bulk component). Since the original interface component (before hydrogenation) has a BE of 60.35 eV, the adsorption-induced shifts can therefore range from 0.15 to 0.45 eV, which is considerably smaller than the shifts in the Pt 4f spectrum for MG/Pt (0.85 eV).

The values of the BE shifts can be used for estimating strength of the C−TM bonds formed upon graphene hydrogenation. This approach is based on the well-known relation between surface core level shifts and the surface energy difference between the Z and Z + 1 metals,[23,24] as applied to adsorbate systems.[25,26] In the framework of the (Z + 1) approximation, the adsorbate-induced BE shifts are proportional to the difference in the metal-adsorbate bond energies for Z and Z + 1 metals:

$$\Delta E_B^Z = \sigma(E^{Z,A} - E^{Z+1,A}) \quad (1)$$

where ΔE_B^Z is the variation in the binding energy of a core electron for the Z metal atom, $E^{Z,A}$ is the energy of the bond between adsorbate atom A and Z metal atom and σ depends on the local adsorbate-to-substrate geometry. Parameter σ can be approximated as $1/n$ for isolated adsorbates, where n is the number of surface atoms to which an adsorbate bonds,[25] and can be set to 1 in the case of atomic H adsorption on graphene. For Pt−C and Ir−C bonds eq 1 transforms to the following:

$$\Delta E_B^{Pt-C} \approx E(Pt - C) - E(Au - C) \quad (2)$$

$$\Delta E_B^{Ir-C} \approx E(Ir - C) - E(Pt - C) \quad (3)$$

Using values of experimental shifts and assuming $E(Au-C) \approx 0$, we estimate $E(Pt-C) \approx 0.85$ eV and $E(Ir-C) \approx 1.0 -1.3$ eV. Therefore, the strength of interaction between the TM substrates and C atoms of graphene is drastically enhanced upon hydrogenation, indicating a transition from the original weak π bonding (sp^2 hybridization) to the formation of strong σ bonds (sp^3 hybridization). We associate this change with destroying the C=C double bonds in graphene upon H adsorption, followed by the engagement of the extra unpaired electrons into the bonding with the substrate.

We return now to the relatively high ratio of sp^3 hybridized carbons in MG/Pt, and the even higher ratio in MG/Ir. Assuming for the moment that the hydrogenation occurs only on the top side of the MG, it is accompanied by the formation of stronger Pt−C respectively Ir−C bonds. The most energetically stable configuration should be the graphane-like constellation, where

every second C atom is bound to a hydrogen and buckled upward while the rest form strong bonds with the substrate and are thus buckled downward. This structure has recently been predicted for hydrogen adsorbed on MG/Ir.[10] It has been found that such bonding to the substrate can occur only on those areas of the surface where every second C atom is situated above a substrate atom, i.e., in the pores of the MG/Ir moiré structure. The C-substrate distance in these graphane-like areas is then also expected to be somewhat shortened as compared to pristine MG/Ir. Thus, the bonding sites (pores) are the first candidates for the formation of the H induced graphane-like structures.

According to this picture, a possible assignment for the components in the C 1s spectra is the following. Peak C1 (around 284 eV) is assigned to the C atoms preserving the sp^2 coordination. Peak C2 (around 285 eV) has a BE similar to that of the C−H component in the HOPG case and therefore it is assigned to the C−H bonds on the elevated nonbonding stripes of graphene (wires). The intensity of peak C3 (around 284.5 eV) correlates with the relative area covered by the bonding sites (pores), being higher for MG/Ir than for MG/Pt. Therefore, we associate C3 with the sp^3-bonded C atoms in the pores, both hydrogenated (buckled upward) and bound to the substrate (buckled downward).

We cannot fully exclude the possibility that some of the hydrogen can intercalate under the graphene layer, however, for a number of reasons we find it unlikely: (i) The fully formed graphane would show only C sp^3 bonds, yet in our spectra a clear sp^2 signal remains at all times. Second, the signature of the measured metal core level spectra is consistent with the increased C-metal bonding. (ii) From PES measurements of metallic clusters (e.g., Ir, Pt, Au) on MG/Ir we observe the same behavior in both the substrate core level as well as the carbon core level, upon cluster formation.[27] Again, this can be explained by an increased interaction between graphene and the underlying substrate. (iii) On H/MG/Pt, no signal consistent with Pt−H bonds is observed, as checked by direct hydrogenation of clean Pt(111). It is interesting to note that intercalation of atomic H does happen at the MG/SiC interface, where H atoms form bonds to the topmost Si atoms, breaking the covalent Si−C interaction between substrate and the buffer layer.[28] In contrast, on noble metals like Pt and Ir, graphene is already preactivated, and the reactive H atoms can readily stick to it in the pores forming a graphane-like structure, making the lengthy process of intercalation through defects less favorable.

The case of H/MG/Ni is very different from H/MG/Pt and H/MG/Ir, because the MG−Ni bonds are already strong and short (~2.1 Å[20,29]) and the interface is lattice matched (e.g., no mismatch-related pores and wires). Figure 5 shows the carbon core level and schematics of MG/Ni before and after hydrogenation. The C 1s spectrum of the initial graphene on Ni(111) consists of a single component (Figure 5a) at 284.8 eV, in accordance with earlier studies.[21,30] The single-component shape of the C 1s peak is somewhat surprising, because carbon atoms are adsorbed on two distinct sites (on top of Ni atoms and in the fcc hollows[20,21]); it can be explained by strong delocalization of electron density between adjacent atoms in the graphene sheet. An additional tiny component at 283.2 eV is attributed to carbon dissolved in the bulk, and since neither its intensity nor the shape changes after hydrogenation, it can be excluded from the discussion. Upon hydrogenation (Figure 5b) two shoulders (c2 and c3) develop on the opposite sides of the original peak (c1), and their contribution to the total C 1s signal reaches 45%. (These components are denoted by small letters in order to distinguish this special case from H/MG/Pt and
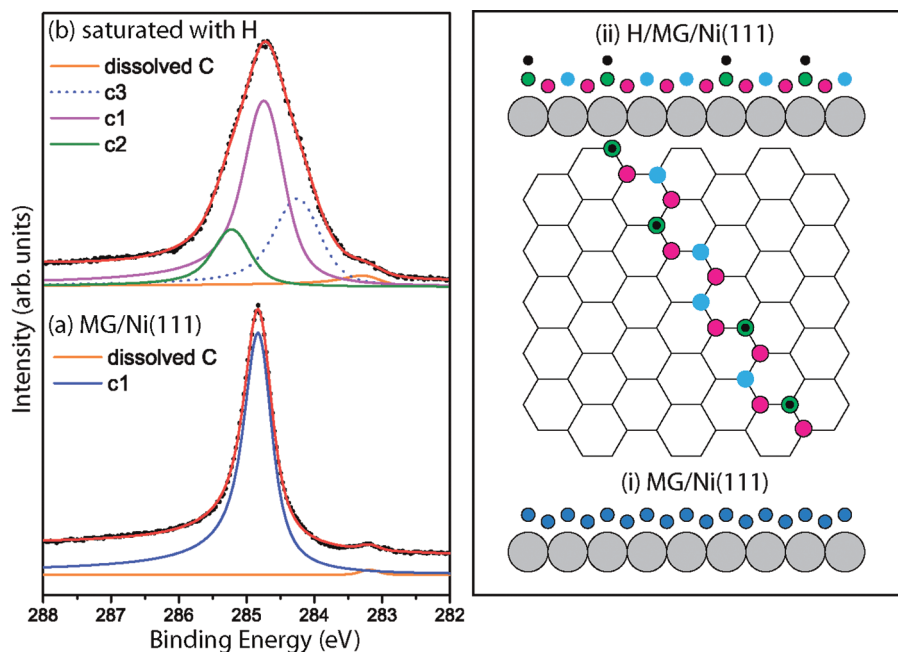
Figure 5. C 1s PES (hν = 400 eV) MG/Ni(111) (a) before and (b) after hydrogenation. The schematics show the MG/Ni (i) lateral view before hydrogenation and (ii) lateral and top view after hydrogenation to saturation.

H/MG/Ir). It is plausible to assign peak c1 to the C atoms above the Ni fcc hollow sites, because these atoms are already buckled downward, and cannot attract hydrogen, which sticks only to the upward buckled atoms in the "on top" positions (above the Ni atoms).[31] This interpretation is supported by the contribution of c1 to the total C 1s intensity (55%), which is close to the fraction of the C atoms in the fcc hollow sites (50%). By analogy with H on HOPG, MG/Pt, and MG/Ir, peak c2 can be associated with the hydrogenated C atoms in the "on top" positions. Evidently, it is impossible to explain the C 1s spectral shape with the formation of a graphane-like layer, which would then result in just two components (c1 and c2) of equal intensity. On the contrary, we observe an intense component c3 at lower BE, which has to be assigned to the non-hydrogenated C atoms in the "on top" positions.

Our explanation of the fact that only a part of the on-top C atoms can accept hydrogen is the following. The adsorption of individual H atom on graphene necessarily breaks the C=C bond and creates an unpaired electron. Saturating this dangling bond on the same graphene sublattice is energetically unfavorable,[4] and is the reason why meta-dimers (1,3-dihydrogenated ring) are less favorable on graphite (0001).[14] In the case of MG/Ni the unpaired electron cannot be transferred to the fcc hollow sublattice because of the strong bonding to the underlying Ni, which makes the barrier for new bond formation very high. Therefore, the unpaired electron remains on the nearest neighbors belonging to the same sublattice (positions 3 and 5 in the C ring assuming the adsorption position is 1). The increased electron density on these positions elevates the barrier for the H adsorption, thus preventing the corresponding on-top C atoms from forming the C—H bonds. The increased electron density on these atoms shifts the corresponding C 1s peak (c3) to lower BEs, in agreement with our experiment. In the schematic drawing of Figure 5 red circles represent the fcc sublattice (c1, prohibited for H adsorption), while green and blue circles stand for the top sublattice. If green sites are hydrogenated (c2), then blue sites cannot be hydrogenated any more (c3). Evidently, the ratio of sites c1:c2:c3 is theoretically limited to 3:1:2 (~50%, 17%, and 33%), but since H adsorption happens randomly the

c2/c3 intensity ratio may be reduced. The experimental intensity ratio of peaks c1, c2, and c3 are fairly close to the above limit, i.e., 55%, 16%, and 29%, respectively.

Conclusions

Graphene's ability to adsorb atomic hydrogen is strongly dependent on the character of the underlying substrate. Without a reactive substrate, the saturated H coverage is relatively low. By adsorption of graphene on a reactive metal substrate, the H uptake value can be increased significantly. At the present hydrogen dosing conditions, the highest values are observed for MG/Ir(111), less for MG/Pt(111), even less for MG/Ni, and the least for the adsorption on bulk graphite. On the lattice-mismatched MG/Pt and MG/Ir interfaces, graphene is slightly corrugated on the nanometer scale inducing site selectivity for H adsorption. The more bonding graphene patches (pores) are able to achieve 50% H coverage by forming graphane-like structures. This process becomes possible due to the strengthening the C $2p_z$-TM 5d bonds, which can involve the unpaired electrons released upon breaking the C=C bonds in the course of H adsorption. The total area of more strongly bonding graphene sites (pores) is higher for MG on Ir than on Pt, thus resulting in the higher H coverage. The nonbonding graphene patches (wires) are much more passive, and hydrogenation of these sites is expected to be similar to that of HOPG. For the already strongly bound and lattice matched interfaces (MG/Ni), no further bond strengthening is possible, and moreover, the hollow site sublattice is excluded from hydrogenation entirely. A graphane-like structure can therefore not be found and the dangling bonds have to be accommodated on the same sublattice (top sites). This produces a strong reduction in the H uptake value, where each formed C—H bond means the blocking of at least two C atoms from further hydrogen adsorption.

References and Notes

(1) Novoselov, K. S.; Geim, A. K.; Morozov, S. V.; Jiang, D.; Katsnelson, M. I.; Grigorieva, I. V.; Dubonos, S. V.; Firsov, A. A. *Nature* **2005**, *438*, 197.

(2) Morozov, S. V.; Novoselov, K. S.; Katsnelson, M. I.; Schedin, F.; Elias, D. C.; Jaszczak, J. A.; Geim, A. K. *Phys. Rev. Lett.* **2008**, *100*, 016602.

(3) Schedin, F.; Geim, A. K.; Morozov, S. V.; Hill, E. W.; Blake, P.; Katsnelson, M. I.; Novoselov, K. S. *Nat. Mater.* **2007**, *6*, 652.

(4) Boukhvalov, D. W.; Katsnelson, M. I. *J. Phys.: Condsens. Matter* **2009**, *21*, 344205.

(5) Zhou, J.; Wang, Q.; Sun, Q.; Chen, X. S.; Kawazoe, Y.; Jena, P. *Nano Lett.* **2009**, *9*, 3867.

(6) Boukhvalov, D. W.; Katsnelson, M. I.; Lichtenstein, A. I. *Phys. Rev. B* **2008**, *77*, 035427.

(7) Boukhvalov, D. W.; Katsnelson, M. I. *Phys. Rev. B* **2008**, *78*, 085413.

(8) Elias, D. C.; Nair, R. R.; Mohiuddin, M. G.; Morozov, S. V.; Blake, P.; Halsall, M. P.; Ferrari, A. C.; Boukhvalov, D. W.; Katsnelson, M. I.; Geim, A. K.; Novoselov, K. S. *Science* **2009**, *323*, 610.

(9) Ferro, Y.; Teillet-Billy, D.; Rougeau, N.; Sidis, V.; Morisset, S.; Allouche, A. *Phys. Rev. B* **2008**, *78*, 085417.

(10) Balog, R.; Jørgensen, B.; Nilsson, L.; Andersen, M.; Rienks, E.; Bianchi, M.; Fanetti, M.; Lægsgaard, E.; Baraldi, A.; Lizzit, S.; Šljivančanin, Ž. Besenbacher, F.; Hammer, B.; Pedersen, T. G.; Hofmann, P.; Hornekær, L., *Nat. Mater.*, DOI:10.1038/NMAT2710.

(11) Sofo, J. O.; Chaudhari, A. S.; Barber, G. D. *Phys. Rev. B* **2007**, *75*, 153401.

(12) Deng, W.-Q.; Xu, X.; Goddard, W. A. *Phys. Rev. Lett.* **2004**, *92*, 166103.

(13) Balog, R.; Jørgensen, B.; Wells, J.; Lægsgaard, E.; Hofmann, P.; Besenbacher, F.; Hornekær, L. *J. Am. Chem. Soc.* **2009**, *131*, 8744.

(14) Hornekær, L.; Šljivančanin, Ž.; Xu, W.; Otero, R.; Rauls, E.; Stensgaard, I.; Lægsgaard, E.; Hammer, B.; Besenbacher, F. *Phys. Rev. Lett.* **2006**, *96*, 156104.

(15) Preobrajenski, A. B.; Ng, M. L.; Vinogradov, A. S.; Mårtensson, N. *Phys. Rev. B* **2008**, *78*, 073401.

(16) Wintterlin, J.; Bocquet, M.-L. *Surf. Sci.* **2009**, *603*, 1841.

(17) Adams D. L. FitXPS (version 2.12). http://www.sljus.lu.se/download.html (accessed May 28, 2009).

(18) Stöhr, J. *NEXAFS Spectroscopy*; Springer: Berlin, 1992.

(19) Nikitin, A.; Näslund, L.-Å.; Zhang, Z.; Nilsson, A. *Surf. Sci.* **2008**, *602*, 2575.

(20) Bertoni, G.; Calmels, L.; Altibelli, A.; Serin, V. *Phys. Rev. B* **2004**, *71*, 075402.

(21) Rusz, J.; Preobrajenski, A. B.; Ng, M. L.; Vinogradov, N. A.; Mårtensson, N.; Wessely, O.; Sanyal, B.; Eriksson, O. *Phys. Rev. B* **2010**, *81*, 073402.

(22) Tanuma, S.; Powell, C. J.; Penn, D. R. *Surf. Interface Anal.* **2005**, *37*, 1.

(23) Johansson, B.; Mårtensson, N. *Phys. Rev. B* **1980**, *21*, 4427.

(24) Johansson, B.; Mårtensson, N. *Helv. Phys. Acta* **1983**, *56*, 405.

(25) Tréglia, G.; Desjonquères, M. C.; Spanjaard, D.; Lassailly, Y.; Guillot, C.; Jugnet, Y.; Duc, T. M.; Lecante, J. *J. Phys. C: Solid State Phys.* **1981**, *14*, 3463.

(26) Dückers, K.; Prince, K. C.; Bonzel, H. P.; Cháb, V.; Horn, K. *Phys. Rev. B* **1987**, *36*, 6292.

(27) J. Knudsen et al., unpublished work.

(28) Riedl, C.; Coletti, C.; Iwasaki, T.; Zakharov, A. A.; Starke, U. *Phys. Rev. Lett.* **2009**, *103*, 246804.

(29) Gamo, Y.; Nagashima, A.; Wakabayashi, M.; Terai, M.; Oshima, C. *Surf. Sci.* **1997**, *374*, 61.

(30) Grüneis, A.; Kummer, K.; Vyalikh, D. V. *New J. Phys.* **2009**, *11*, 073050.

(31) Sha, X.; Jackson, B. *Surf. Sci.* **2002**, *496*, 318.